

20 ABSTRACT

21 Drinking water treatment residuals (DWTRs) are a promising media amendment for
22 enhancing phosphorus (P) removal in bioretention systems, but substantial removal of dissolved
23 P by DWTRs has not been demonstrated in field bioretention experiments. We investigated the
24 capacity of a non-amended control media (Control) and a DWTR-amended treatment media
25 (DWTR) to remove soluble reactive P (SRP), dissolved organic P (DOP), particulate P (PP), and
26 total P (TP) from stormwater in a two-year roadside bioretention experiment. Significant
27 reductions in SRP, PP and TP concentrations and loads were observed in both the Control and
28 DWTR media. However, the P removal efficiency of the DWTR cells were greater than those of
29 the Control cells for all P species, particularly during the second monitoring season as P sorption
30 complexes likely began to saturate in the Control cells. The difference in P removal efficiency
31 between the Control and DWTR cells was greatest during large storm events, which transported
32 the majority of dissolved P loads in this study. We also investigated the potential for DWTRs to
33 restrict water flow through bioretention media or leach heavy metals. The DWTRs used in this
34 study did not affect the hydraulic performance of the bioretention cells and no significant
35 evidence of heavy metal leaching was observed during the study period. Contrasting these results
36 with past studies highlights the importance of media design in bioretention system performance
37 and suggests that DWTRs can effectively capture and retain P without affecting system
38 hydraulics if properly incorporated into bioretention media.

39 KEY WORDS: *bioretention, drinking water treatment residuals, phosphorus removal, hydraulic*
40 *conductivity, heavy metals, field study*

41

42

43 INTRODUCTION

44 Urban landscapes contain substantial amounts of phosphorus (P) originating from lawn
45 fertilizer, pet waste, soil particles, plant litter and atmospheric deposition (Hobbie et al. 2017;
46 Müller et al. 2020; U.S. EPA 1999). The transport of urban P sources to surface waterbodies via
47 runoff is a leading cause of eutrophication and harmful algal blooms in freshwater ecosystems
48 (Carpenter et al. 1998; National Research Council 2009; U.S. EPA 2009). Bioretention systems
49 are a form of green stormwater infrastructure increasingly used in developed areas for hydrologic
50 control and water quality improvement (Davis et al. 2009; Taguchi et al. 2020). While
51 bioretention systems have proven effective for reducing peak flow rates, sediment loads, and
52 concentrations of certain pollutants (LeFevre et al. 2015; Liu et al. 2017; Vijayaraghavan et al.
53 2021), their capacity to remove P from stormwater is highly variable and some studies have even
54 shown net release of P (Cording et al. 2018; Dietz and Clausen 2005; Hatt et al. 2009; Hunt et al.
55 2006; Shrestha et al. 2018)

56 Because P does not have a gaseous phase relevant in the context of stormwater
57 (Schlesinger and Bernhardt 2013), the long-term P removal performance of bioretention systems
58 depends on their ability to retain the P that passes through them. Bioretention P removal
59 effectiveness varies across the chemical species of P (Liu and Davis 2014). While conventional
60 bioretention media constituents (e.g. sand, compost, topsoil) effectively filter particulate P (PP),
61 they have limited capacity to adsorb dissolved P (Li and Davis 2016; Tirpak et al. 2021).
62 Consequently, dissolved organic P (DOP) and dissolved inorganic P (measured as soluble
63 reactive P; SRP) can pass through bioretention systems in solution as P sorption complexes
64 saturate. Long-term P retention is further complicated by leaching of dissolved P from organic
65 media substrates and mineralization of P from plant litter and trapped organic sediments (Chahal

66 et al. 2016; Hurley et al. 2017; LeFevre et al. 2015; Passeport et al. 2009). Novel media designed
67 specifically for P retention is therefore needed for bioretention systems to capture and retain P
68 over decadal timeframes that match anticipated system lifespans.

69 P retention can be enhanced in bioretention systems by amending the soil media with P-
70 sorbing materials (Marvin et al. 2020). Many industrial byproducts contain high concentrations
71 of metal hydroxides, which can bind dissolved P through chemical adsorption or precipitation
72 processes (Buda et al. 2012; Cucarella and Renman 2009; Leader et al. 2008). Incorporating
73 these materials into bioretention systems may reduce P entering water bodies via stormwater
74 runoff, and subsequently reduce eutrophication, while also representing an opportunity to
75 beneficially reuse waste products that municipalities would otherwise pay to landfill (Babatunde
76 and Zhao 2007). Drinking water treatment residuals (DWTRs) are a byproduct of the drinking
77 water treatment process and have promise as a bioretention amendment due to their widespread
78 availability, low cost, and high P sorption capacity (Babatunde et al. 2009; Ippolito et al. 2011;
79 O'Neill and Davis 2011a). P sorption by aluminum (Al)-based DWTRs is relatively insensitive
80 to soil redox conditions (Penn and Bowen 2018; Zvomuya et al. 2006), which allows them to
81 retain P despite any fluctuations in oxygen availability. Furthermore, incorporating Al-DWTRs
82 into bioretention media has potential to reduce urban P loads in cold climates where biological P
83 uptake mechanisms are dormant during late fall to early spring months.

84 Many studies have demonstrated enhanced removal of dissolved P by DWTR-amended
85 bioretention media in laboratory column experiments (Liu et al. 2014; Lucas and Greenway
86 2011; O'Neill and Davis 2011b; Palmer et al. 2013; Poor et al. 2018; Yan et al. 2016b), but these
87 results have not been adequately validated in the field. In fact, a recent review of P-sorbing
88 amendments in bioretention media by Marvin et al. (2020) identified only two unique field

89 installations (results presented in Liu and Davis (2014), Roseen and Stone (2013), and Houle
90 (2017)) that have evaluated the P removal performance of DWTRs in urban bioretention. In both
91 of these installations, the DWTR-amended media failed to significantly reduce stormwater SRP
92 concentrations, despite effective SRP removal in corresponding column experiments (O'Neill
93 and Davis 2011b; Roseen and Stone 2013). Liu and Davis (2014) also investigated the potential
94 for DWTRs to retain DOP but did not observe significant DOP removal. Authors speculated that
95 poor dissolved P removal performance was due to equilibrium adsorption dynamics (Liu and
96 Davis 2014), short-circuiting of the media volume (Roseen and Stone 2013), and non-uniform
97 distributions of DWTRs in the filter media (Roseen and Stone 2013). Further research is needed
98 to establish whether DWTRs can, in fact, enhance dissolved P removal in field contexts and to
99 determine the factors that regulate P removal by DWTRs in urban bioretention systems.

100 Another dimension of adding DWTRs to bioretention media is whether this practice
101 produces unintended consequences. The high P sorption capacity of DWTRs has been linked to
102 their large surface areas and fine-grained texture (Ament et al. 2021; Yang et al. 2006), which
103 could cause flow restrictions in DWTR-amended media. Ament et al. (2021) and Yan et al.
104 (2017) demonstrated that additions of DWTRs to bioretention media can reduce infiltration rates
105 in column experiments. Such hydraulic restrictions in field contexts could produce preferential
106 flow paths that facilitate media short-circuiting or clogging of outlets that lead to excessive
107 ponding or backflow.

108 Additionally, DWTRs can contain high concentrations of heavy metals (Buda et al. 2012;
109 Ippolito et al. 2011), which could potentially leach from bioretention systems amended with
110 these materials and pose risks to surface and ground water resources. Metals, such as Al,
111 manganese (Mn), and zinc (Zn), can be toxic to humans and aquatic life and have been shown to

112 leach from DWTRs in column studies (Mortula and Gagnon 2007; Novak et al. 2007; Palmer et
113 al. 2013). However, urban runoff can contain heavy metals such as arsenic (As) and cadmium
114 (Cd) (Davis et al. 2001), which some P-sorbing materials can adsorb (Lim et al. 2015; Siswoyo
115 et al. 2014; Zhou and Haynes 2012). The potential leaching of heavy metals from industrial
116 byproducts is a common concern that limits broader use of DWTRs in field applications (Ippolito
117 et al. 2011), yet few studies have investigated heavy metal dynamics in field bioretention
118 systems amended with DWTRs.

119 Here, we conducted a two-year experiment to investigate the potential for AI-DWTRs to
120 enhance the P removal performance of bioretention systems under field conditions. This study
121 builds upon a previous laboratory study by Ament et al. (2021), which developed design
122 recommendations for balancing hydraulic control and P removal in DWTR-amended
123 bioretention media. Results from that study indicated that mixing DWTRs with sand and placing
124 them beneath a surface layer of mixed sand and “low-P” compost can provide long-term (> 10
125 years) P retention, while alleviating hydraulic restrictions imposed by fine-grained DWTRs.
126 However, laboratory studies cannot account for natural variations in temperature, hydraulic
127 loading, stormwater chemistry and other environmental factors, so field experiments are needed
128 to validate laboratory results. The objectives of this study were therefore to:

- 129 a) Investigate the capacity of a bioretention media amended with DWTRs to retain SRP,
130 DOP and PP in field contexts
- 131 b) Explore the drivers of P removal in bioretention systems with and without DWTRs
- 132 c) Determine whether a mixed layer of sand and DWTRs affects bioretention system
133 hydraulics under variable field conditions
- 134 d) Assess the potential for DWTRs to leach or adsorb heavy metals (Al, As, Cd, Mn, Zn)

135 MATERIALS AND METHODS

136 **Site Description**

137 This study was conducted at the University of Vermont (UVM) Bioretention Laboratory,
138 which is situated along a road that services a major parking lot on the UVM campus in
139 Burlington, VT. The site contains eight equally sized bioretention cells (3.7 m² area, 1 m depth)
140 that receive stormwater inputs from drainage areas of varying sizes (Cording et al. 2018). Lined
141 swales covered in gravel (3-5 cm diameter) convey runoff from the asphalt through a curb cut
142 into the bioretention cells. Each bioretention cell is fitted with an impermeable rubber liner,
143 which prevents water exchange with the surrounding soil and allows for mass balance
144 calculations. Each bioretention cell contains a perforated underdrain raised approximately 12 cm
145 above the bottom of the cell, which creates a small internal water storage zone.

146 **Experimental Design**

147 A field bioretention experiment was conducted to compare differences in water quality
148 improvement between a DWTR-amended treatment media and a non-amended control media
149 (henceforth referred to as “DWTR” and “Control”, respectively). In May 2019, four existing
150 bioretention cells were excavated. Two of these cells were retrofitted with the Control media,
151 while the remaining two cells were retrofitted with the DWTR media. To account for potential
152 hydrologic variability, the bioretention cells were grouped by the relative size of their drainage
153 areas and randomly assigned the Control or DWTR media. One group of cells consisted of 43 m²
154 and 32 m² drainage areas (henceforth referred to as the “Small Drainage Area Control” cell and
155 the “Small Drainage Area DWTR” cell, respectively), while the other group consisted of 59 m²
156 and 54 m² drainage areas (henceforth referred to as the “Large Drainage Area Control” cell and
157 the “Large Drainage Area DWTR” cell, respectively).

158 The Control media contained washed gravel (3-5 cm diameter), washed pea stone (1-2
159 cm diameter), washed sand (< 2 mm diameter) and compost (Figure 1a). Previous research has
160 shown that conventional bioretention media (e.g., 60% sand, 40% compost) and composts
161 derived from manure feedstocks leach nutrients into bioretention effluent (Cording et al. 2017,
162 2018; Mullane et al. 2015). Accordingly, the Control media in this study contained reduced
163 quantities (10% compost by volume in the top 30.5 cm of media) of a low-P compost (derived
164 from leaf litter feedstocks; 0.19% P by dry mass) (Shrestha et al. 2020) to limit the internal P
165 content of the media. The DWTR media was identical to the Control, except that 10% of the
166 sand layer (located 30.5 cm – 71 cm below the media surface) volume was replaced with
167 DWTRs (Figure 1b), which Ament et al. (2021) determined to be enough for long-term (> 10
168 years) P removal. The DWTRs were passed through a 5 mm sieve to remove coarse debris and
169 mixed into the sand with cement mixers. The DWTRs used in this study were obtained from the
170 University of New Hampshire Water Treatment Plant (Durham, NH), which uses polyaluminum
171 chloride as a treatment coagulant and processes its DWTRs via freeze-thaw cycling. This
172 material exhibited the lowest P retention capacity of the three DWTR sources evaluated in
173 Ament et al. (2021) and was selected for this study to provide a conservative estimate of the P
174 removal performance of DWTRs in field bioretention systems. A summary of the physical and
175 chemical properties of this DWTR material is provided in Table S1.

176 After retrofit, all four cells were planted with an identical assemblage of species, which
177 consisted of *Asclepias tuberosa* (Butterfly Milkweed, $n=1$ plant per bioretention cell), *Echinacea*
178 *purpurea* (Echinacea Sp., $n=2$), *Helenium autumnale* (Sneezeweed ‘Sombbrero’, $n=1$), *Iris*
179 *versicolor* (Harlequin Blueflag, $n=3$), and *Symphotrichum nova-angliae* (New England Aster,
180 $n=2$). Vegetation was watered every other day for three weeks to ensure plant establishment. The

181 *Helenium autumnale* cultivar did not survive the first season of study and was replaced with
182 *Zizia aurea* (Golden Alexander) in May of 2020.

183 **Stormwater Sampling**

184 Stormwater inflows and outflows from the four bioretention cells were simultaneously
185 monitored with eight autosamplers (Teledyne ISCO 6712, Lincoln, NE). A cedar box equipped
186 with a 90° v-notch weir was placed at the inlet of each bioretention cell to capture runoff being
187 conveyed from the road (Figure 2, left). Inflow volumes were determined using submerged probe
188 flow modules (ISCO 720) to measure the stage height of water within the weir boxes (Cording et
189 al. 2017) every minute. Stage height measurements were converted to flow rates using the
190 equation (Dunne and Leopold 1978):

$$191 \quad L/s = 1380 (\text{stage height m})^{2.5}$$

192 Outflow volumes were determined similarly. However, instead of using a weir box to
193 measure flow, a sealed sump was used, which drained into a 15 cm diameter PVC pipe equipped
194 with a Thel-Mar weir (Thel-Mar, LLC, Brevard, NC) (Figure 2, right). Submerged probes
195 secured to the bottom of the sumps were used to measure stage heights, which were converted to
196 flow rates using conversion charts provided by Thel-Mar, LLC.

197 Flow-based composite sampling (fifteen 200 ml water samples per bottle) was used to
198 monitor inflow and outflow stormwater quality for the bioretention cells. For a given rainfall
199 event, a maximum of four composite water sampling bottles were obtained from each of the
200 inflow and outflow autosamplers, roughly targeting the rising, peak, and falling limbs of the
201 storm hydrograph. The volumetric sampling intervals (L) needed to capture the entire storm
202 event were calculated from rain forecasts before every storm using unique linear relationships
203 between precipitation depth and runoff volume established for each bioretention cell. The weir

204 boxes were cleaned and the autosamplers were zeroed before every storm. Storms were sampled
205 from September to November in 2019, post-plant establishment, and June to November in 2020.
206 The water quality data therefore represent the P removal performance of newly constructed
207 bioretention cells (data from approximately 0.5- and 1.5- years post media retrofit). Furthermore,
208 runoff produced from snowmelt or winter rainfall events was not monitored in this study, so the
209 water quality data only reflects warm weather performance. Every storm forecasted to produce >
210 5 mm of rainfall was monitored with the autosamplers, but only storms that generated outflow in
211 all bioretention cells were analyzed in this study. Twenty-one captured storm events generated
212 outflow during the 2019 and 2020 field monitoring seasons (Table S2).

213 **Water Quality Analysis**

214 All water samples were retrieved from the field within 24 hours of the start of each storm
215 event and processed at UVM's Agriculture and Environmental Testing Laboratory. Total P
216 samples were refrigerated for < 1 week before persulfate digestion and dissolved P samples were
217 filtered through a .45 μm mesh filter and frozen for holding. Samples were analyzed for total P
218 (TP), total dissolved P (TDP) and SRP following standard methods procedures 4500-PE and
219 4500-PJ (Table S3) (APHA et al. 2005). PP and DOP were calculated as TP minus TDP and
220 TDP minus SRP, respectively (Table S3). Method blank corrections were applied to the TP and
221 TDP data to account for potential error introduced by persulfate digestion. A value of half the
222 detection limit was used for any measurements that registered below the detection limits (Davis
223 2007; Liu and Davis 2014). To investigate the effects of data below detection limits, results were
224 assessed assuming concentrations of 0, 0.5, and $1 \times$ detection limits when sample concentrations
225 registered below detection. Results assuming $0.5 \times$ detection limits are presented in all tables and
226 figures in the main article. Results assuming 0 and $1 \times$ detection limits are presented briefly in

227 Tables S4 and S5 and used to provide an estimate of uncertainty driven by low sample
228 concentrations. Additionally, small measurement errors can produce negative PP and DOP
229 values when water samples are dominated by SRP (e.g., outflow samples). To eliminate negative
230 concentrations in the data set, we replaced TDP values with SRP values for cases when TDP <
231 SRP. Similarly, we replaced TP values with TDP values for cases when TP < TDP.

232 Inflow and outflow concentrations of dissolved aluminum (Al), arsenic (As), cadmium
233 (Cd), manganese (Mn) and zinc (Zn) were also analyzed for four storms during the 2019
234 monitoring season and six storms during the 2020 monitoring season. These metals were selected
235 due to their potential prevalence in DWTRs and urban stormwater (Grebel et al. 2013; Ippolito et
236 al. 2011; Steele et al. 2015; Zhao and Yang 2010), as well as their threat to human and aquatic
237 life. After P samples were collected from the sampling bottles of each autosampler, a heavy
238 metal sample was obtained by pouring the remaining water contents of the sampling bottles into
239 a churn splitter and mixing the water to generate one flow-weighted composite sample. These
240 heavy metal samples were filtered through a .45 μm filter, preserved with nitric acid (HNO_3), and
241 analyzed using inductively coupled plasma mass spectrometry (for As) and optimal emission
242 spectrometry (for Al, Cd, Mn and Zn) methods at an external chemistry lab (Endyne, Inc.,
243 Williston, VT).

244 **Hydrologic and Water Quality Calculations**

245 Total flow volumes (V) were calculated for each storm by summing the product of the
246 instantaneous flow rate (Q(t)) and the flow measurement time interval (Δt) for the entire runoff
247 period:

$$248 \quad V = \sum Q(t) \Delta t$$

249 P load masses (M) were calculated for each storm by summing the product of the
250 autosampler bottle P concentrations (C_i) and their corresponding runoff volumes (V_i):

$$251 \quad M = \sum C_i V_i$$

252 Heavy metal loads were determined by multiplying the concentration of the single flow-weighted
253 composite sample by the total flow volume (V).

254 When precipitation depths far-exceeded forecasted depths, the programmed volumetric
255 sampling intervals were not broad enough to capture the entire storm event. In the four instances
256 where this occurred, we applied P concentrations from the last sampling bottle to the unsampled
257 portion of the flow volume, which ranged from 1% to 44% of the total runoff volume.

258 Event mean concentrations (EMC) were calculated for each storm by dividing the total
259 load masses (M) by the total flow volumes (V):

$$260 \quad EMC = M / V$$

261 P mass removal efficiency expressed in percentage were calculated as:

$$262 \quad \text{Removal efficiency (\%)} = ((M_{in} - M_{out}) / M_{in}) \times 100$$

263 Positive values indicate a net retention of P, while negative values indicate a net export of P.

264 The percentage of P mass load reductions attributable to volume reductions (LR_{vol}) was
265 calculated as:

$$266 \quad LR_{vol} = [(V_{in} - V_{out}) \times EMC_{out} / M_{in}] \times 100$$

267 The percentage of P mass load reductions attributable to concentration reductions (LR_{conc}) was
268 calculated as $100 - LR_{vol}$.

269 Hydraulic detention times were calculated for each storm event by the time difference
270 between the center of mass of the inflow and outflow hydrographs (Barfield et al. 1981).
271 Hydrograph centers of mass were defined as the point at which half of the total stormwater

272 volume had flowed into or out of the bioretention cell. Peak flow ratios (R_{peak}) were also
273 determined for each bioretention cell and storm event and were calculated as the maximum
274 outflow rate divided by the maximum inflow rate (Davis 2008). Hydraulic detention time and
275 R_{peak} values were used to assess bioretention system hydraulics.

276 **Statistical Methods**

277 Statistical analyses were performed to assess water quality differences between paired
278 inflow and outflow data for each bioretention cell. Separate storm events were considered
279 replicates for statistical purposes (Shrestha et al. 2018; Winston et al. 2013) and were identified
280 by inter-storm dry periods of at least 12 hours. Storm events were only included in this analysis
281 when inflow and outflow volumes were accurately measured in all four bioretention cells. The
282 paired difference data failed multiple goodness-of-fit tests for normality (i.e. Shapiro-Wilk,
283 Kolmogorov-Smirnov), so a non-parametric Wilcoxon Signed Rank test was used to evaluate
284 differences between inflow and outflow volumes, nutrient loads, and concentrations (Shrestha et
285 al. 2018). A non-parametric Kruskal-Wallis test was used to assess differences in hydraulic
286 detention time and R_{peak} values between the bioretention cells. All statistical analyses were
287 performed in R (R Core Team 2016).

288 **RESULTS**

289 **Captured Storms and Flow Volumes**

290 Eight and thirteen distinct storm events were captured in the 2019 and 2020 field
291 monitoring seasons, respectively (Table S2). During these events, the two Control and two
292 DWTR bioretention cells received combined totals of 99,500 L and 90,500 L of stormwater,
293 respectively (Table 1). Although the experimental groups (Control and DWTR) received similar
294 aggregate inflow volumes, the Small Drainage Area DWTR cell received 20% more inflow than

295 the Small Drainage Area Control cell and the Large Drainage Area DWTR cell received 35%
296 less inflow than the Large Drainage Area Control cell (Table 1). Stormwater outflow volumes
297 were significantly less than inflow volumes for all cells monitored in this study ($p < 0.01$).
298 Overall, the Small Drainage Area Control and DWTR cells reduced stormwater flow volumes by
299 46% and 45%, while the Large Drainage Area Control and DWTR cells reduced volumes by
300 26% and 52%, respectively (Table 1).

301 **Stormwater P Species Composition and Removal**

302 Influent TP was composed of 43% SRP, 5% DOP, and 52% PP on average. Median
303 concentrations of SRP, DOP and PP were $0.022 \text{ mg P L}^{-1}$, $0.002 \text{ mg P L}^{-1}$, and $0.036 \text{ mg P L}^{-1}$,
304 respectively. These values came from a university campus roadway and are lower than the SRP,
305 PP and TP values typically reported in urban bioretention studies (Dietz and Clausen 2005; Hunt
306 et al. 2006; Komlos and Traver 2012; O'Neill and Davis 2011a; Shrestha et al. 2018).
307 Additionally, average influent SRP concentrations in 2020 were 76% lower than those of 2019,
308 which could be due to having sampled more summer storms (which are less influenced by leaf
309 litter P loads than fall storms) in 2020 than 2019, or decreased road traffic due to COVID-19
310 restrictions. Stormwater DOP concentrations are rarely analyzed, but the influent DOP
311 concentrations measured in this study were nearly an order of magnitude lower than those
312 reported by Liu and Davis (2014) and Song et al. (2015). All of the bioretention cells in this
313 study functioned to significantly decrease both P concentrations and loads for SRP, PP and TP (p
314 < 0.01 ; Figures 3 and 4). Significant reductions in DOP concentrations and loads were not
315 observed in any cell ($p > 0.1$), but DOP concentrations were very low in both inflows and
316 outflows (91% of samples registered below 0.01 mg P L^{-1}).

317 While all bioretention cells demonstrated significant capacity to remove P, the DWTR
318 cells exhibited better P removal performance than the Control Cells for all P species (Figure 5;
319 Table 1). The 2-year total mass removal efficiency values for TP were 91% and 79% for the
320 Small and Large Drainage Area Control cells, but 97% and 95% for the Small and Large
321 Drainage Area DWTR cells, respectively (Table 1). This difference in TP removal between the
322 Control and DWTR cells was driven primarily by a major drop in SRP mass removal efficiency
323 for the Control cells relative to the DWTR cells in the second (2020) monitoring season (Figure
324 5). During this period, the Control cells retained 30%-80% of SRP loads, while the DWTR cells
325 retained 91%-93% of SRP loads (Table 1). Differences in P removal performance between the
326 Control and DWTR cells also grew for PP during the 2020 monitoring season (Table 1).

327 In this study, water quality samples considered below the detection limits ranged from
328 20%-29% of the data, depending on the P species (Table S6). Outflow samples accounted for the
329 majority (>80%) of samples below detection and non-detects accounted for a larger proportion of
330 outflow samples for DWTR cells than Control cells. Compared to assigning non-detects a value
331 of 0.5× detection limits, the 0 or 1× detection limits approaches slightly altered the 2-year mass
332 removal efficiency values for SRP, PP, and TP by 0.5% – 2.0% across all bioretention cells
333 (Tables S4 and S5). Further, statistical outcomes were uniform across the 0, 0.5, and 1× detection
334 limits scenarios for these P species. However, for DOP, detection limit assumptions altered the
335 2-year mass removal efficiency values by 12%-42% and changed statistical outcomes for all
336 bioretention cells, likely because DOP concentrations were extremely low in this study (Tables
337 S5 and S6). Accordingly, future study is needed to confirm whether these low concentrations are
338 typical and assess DOP removal performance of bioretention.

339

340 **Role of Volume Reductions, Concentration Reductions, and Storm Size in P Removal**

341 The observed P load reductions were due to both stormwater volume reductions (LR_{vol})
342 and P concentration reductions (LR_{conc}). However, LR_{conc} values far surpassed LR_{vol} values for
343 all bioretention cells and P species (Table S7), indicating that P concentration reductions were
344 the primary driver of P load reductions. Although the proportion of total load reductions
345 attributable to concentration reductions were high for both media treatments (63% - 99%), the
346 DWTR cells exhibited higher LR_{conc} values than the Control cells for all P species (Table S7).

347 Storm size also influenced P removal dynamics in this study. Both the Control and
348 DWTR cells exhibited uniformly high mass removal efficiency for all P species during small
349 storm events (rainfall < 25 mm; $n=17$) (Figure S1). However, removal efficiency values dropped
350 substantially for the Control cells during the few large storms (rainfall > 2.5 mm; $n=4$) but
351 remained relatively consistent across storm sizes for the DWTR cells (Figure S1).

352 **Hydraulic Detention Times and Peak Flow Ratios**

353 The addition of DWTRs to bioretention media did not affect system hydraulics in this
354 study. Hydraulic detention times for the bioretention cells were not statistically different from
355 one another ($p > 0.1$), exhibiting median values of 60-65 minutes for the Control cells and 49-67
356 minutes for the DWTR cells. Peak flow ratios (R_{peak}) for the bioretention cells were also not
357 statistically different from one another ($p > 0.1$), exhibiting median values of 0.15-0.19 for the
358 Control cells and 0.17-0.19 for the DWTR cells. The hydraulic detention time and peak flow data
359 are displayed in Figure 6 and Figure 7, respectively.

360 **Stormwater Heavy Metal Composition and Removal**

361 No evidence of heavy metal leaching from, or adsorption by, DWTRs was observed
362 during the study period. The concentration of heavy metals in bioretention inflows and outflows

363 were very low for all cells, with nearly all samples registering below the detection limit for As,
364 Cd, and Mn (Figure 8). Outflow concentrations of Al were slightly higher than inflow
365 concentrations for both media treatments, but outflow Al concentrations were not statistically
366 different than inflow concentrations for any bioretention cell (Figure 8a; $p > 0.1$). Inflow
367 concentrations of Zn registered above the detection limit more than other metals, but outflow Zn
368 concentrations were below the detection limit for all bioretention cells, regardless of DWTR
369 presence.

370 DISCUSSION

371 **P Removal Performance**

372 Our findings reveal that amending bioretention media with DWTRs can enhance P
373 removal from stormwater in field settings. Overall, the DWTR cells received larger P inputs and
374 released smaller P outputs than the Control cells for all P species (Figure 5, Table 1). The
375 difference in P mass removal efficiency between the Control and DWTR cells was greater for
376 dissolved P than particulate P (Table 1), which suggests that the enhanced P sorption capacity of
377 the DWTR media was responsible for the improved P removal performance. While SRP removal
378 efficiency values dropped by 16% and 59% between the 2019 and 2020 sampling seasons for the
379 Small and Large Drainage Area Control cells, respectively, SRP removal efficiency values
380 dropped by only 5% and 3% over the same period for the Small and Large Drainage Area
381 DWTR cells, respectively, despite receiving greater SRP inputs (Table 1). These results suggest
382 that the P sorption complexes of the Control cells became saturated much faster than those of the
383 DWTR cells. Additionally, these results reflect P dynamics in newly retrofitted bioretention
384 systems that experienced relatively small stormwater inflow volumes and low P concentrations.
385 The gap in SRP removal performance between the Control and DWTR media will likely expand

386 with time as the Control cells accumulate P and approach P saturation more rapidly than the
387 DWTR cells. The drop in SRP mass removal efficiency observed between 2019 and 2020 for the
388 Large Drainage Area Control cell provides early evidence of this dynamic, as its P sorption
389 complex likely became more saturated than that of the Small Drainage Area Control cell due to
390 greater P inputs (Table 1). Longer-term field studies are needed to clarify the longevity of P
391 removal for both the Control and DWTR media designs.

392 The DWTR cells also exhibited higher removal efficiency values than the Control cells
393 for DOP and PP. Over the course of the study, the Control cells removed 60%-72% of DOP
394 loads while the DWTR cells removed 77%-93% of DOP loads (Table 1). DOP retention by
395 DWTRs has been demonstrated in previous laboratory column studies (Yan et al. 2016a), but not
396 in field bioretention studies (Liu and Davis 2014). The greater DOP removal efficiency values of
397 the DWTR cells compared to the Control cells is likely due to increased P binding site
398 availability in the DWTR media. However, inflow and outflow concentrations of DOP were very
399 low in this study (Table 1), possibly due to the scarcity of organic matter in the bioretention
400 media as well as 100% paved drainage areas with little surrounding vegetation or sediment
401 sources. Statistically significant DOP removal was not found in any of the bioretention cells
402 (Figure 3) and assumptions regarding below detection limit samples strongly influenced the
403 magnitude of DOP loads. Consequently, strong conclusions regarding the impact of DWTRs on
404 field DOP removal cannot be made. DWTRs were not expected to increase PP removal in this
405 study because sand has been shown to effectively filter suspended solids and particulate matter in
406 past studies (Cording et al. 2018; Davis 2007; Liu and Davis 2014; Roseen and Stone 2013;
407 Shrestha et al. 2018). Nevertheless, the DWTR cells exhibited higher PP mass removal
408 efficiency than the Control cells, particularly in 2020 (Table 1). DWTRs may enhance PP

409 retention by improving particulate filtration or by curbing colloidal migration within sand layers.
410 Future research should investigate whether DWTRs affect physical filtration mechanisms or the
411 movement of fine particles within bioretention media.

412 Although the DWTR cells showed better P retention than the Control cells, P removal by
413 the Control cells was also high compared to other field bioretention studies (Cording et al. 2018;
414 Dietz and Clausen 2005; Hunt et al. 2006; Shrestha et al. 2018). Over the course of the study, the
415 Control cells exhibited combined mass removal efficiency of 84% and 82% for TP and SRP
416 (Table 1), respectively, and never released effluent that exceeded 0.025 mg SRP L⁻¹ (Figure 3).
417 Effective dissolved P removal performance by the Control cells is noteworthy because many
418 field studies have reported substantial net exports of dissolved P from conventional bioretention
419 media (Dietz and Clausen 2005; Hatt et al. 2009; Hunt et al. 2006), including two studies
420 previously conducted in the exact hydrologic locations of the Control cells (Cording et al. 2018;
421 Shrestha et al. 2018). Other than slight variation in plant composition, the only difference
422 between the media of previous studies conducted at the UVM Bioretention Laboratory and the
423 Control media in this study was the compost: the Control media in this study used a smaller
424 amount of compost (10% versus 40% compost by volume in the top 30.5 cm of media) and used
425 compost derived from low P feedstocks (leaf litter), rather than higher P feedstocks (food and
426 animal waste) (Cording et al. 2018; Shrestha et al. 2018). The high P retention performance of
427 the Control cells in this study shows that compost selection criteria (quantity and type) for
428 bioretention media designs can have significant impacts on bioretention nutrient removal
429 performance, especially in settings where P-sorbing amendments are not used or available.

430 **Drivers of P Removal**

431 Because P load reductions can be achieved through volume reductions (e.g. infiltration
432 and water absorption by media) and concentration reductions (e.g. chemical adsorption,
433 precipitation, and biological uptake) in bioretention systems, both mechanisms must be
434 accounted for to isolate the impact of media designs on system performance (Liu and Davis
435 2014). Unlike other bioretention studies that have achieved P load reductions through stormwater
436 volume reductions (Li and Davis 2009; Liu and Davis 2014), P concentration reductions were
437 the primary driver of P removal for all P species in this study. While both the Control and
438 DWTR cells reduced the concentration of P species in stormwater, effluent P concentrations
439 were lower (Table 1) and LR_{conc} values were higher (Table S7) in the DWTR cells for all P
440 species. These results indicate that concentration reductions played a larger role in dissolved P
441 removal for the DWTR cells, consistent with results from prior column studies (Ament et al.
442 2021).

443 Because bioretention cells were lined in this study, stormwater volume reductions were
444 only due to absorption by the soil media and evapotranspiration (ET). ET likely had negligible
445 direct effects on stormwater volumes during storm events, but may have indirectly affected
446 outflow volumes between storms by reducing the volumetric water content and thus increasing
447 the water holding capacity of the soil media (Mullane et al. 2015; Zinger et al. 2021). Although
448 total stormwater volume reductions were fairly high in this study (26%-52%) (Table 1), LR_{vol}
449 values were relatively low (1%-37%) (Table S4). Concentration reductions were the dominant P
450 removal mechanism in this study because effluent P concentrations were much lower than
451 influent P concentrations for all bioretention cells and P species (Table 1).

452 Storm size also influenced P removal performance of the bioretention cells, as Control
453 cells exhibited lower removal efficiency values than DWTR cells during large storms for all P

454 species (Figure S1). Large storms can contribute disproportionately to annual urban P loads
455 (Shrestha et al. 2018), with four large storms (17% of the captured storms) transporting 59% of
456 total inflow SRP loads in this study. P removal also tends to be worse in bioretention systems
457 during large storms than small storms, with some systems exhibiting substantial dissolved P
458 export during large events (Shrestha et al. 2018). The capacity of DWTR-amended media to
459 effectively remove dissolved and particulate P via P concentration reductions during large storm
460 events is particularly relevant for stormwater practitioners seeking to reduce the required areal
461 footprint of bioretention systems, while maintaining P removal performance, in urban areas
462 where compacted soils and liners prevent infiltration.

463 Despite high P removal by the DWTR cells in this study, P retention was not as effective
464 as in prior column studies (Ament et al. 2021). The small discrepancy between lab and field
465 results in this research may be due to a variety of environmental factors. First, the lab experiment
466 did not include plants, which can facilitate preferential flow along their root networks (Muerdter
467 et al. 2016, 2018) and allow a portion of the stormwater to bypass the media. Second, prolonged
468 antecedent dry periods in the field can reduce media contact times by increasing the hydraulic
469 conductivity of bioretention media (Blecken et al. 2009; Hatt et al. 2009). Antecedent dry
470 periods and wetting and drying cycles were not simulated in the Ament et al. (2021) column
471 study, so it is unclear whether these factors affect P removal by DWTRs. Finally, field SRP
472 inflow concentrations exhibited a median value of 0.022 mg P L⁻¹ compared to the 0.2 mg P L⁻¹
473 used in the column study. Because sorption processes are driven by equilibrium dynamics
474 (Ament et al. 2021; Li et al. 2016), very low influent P concentrations could suppress P sorption
475 and even favor P desorption in the field. Any combination of these factors could explain the

476 small discrepancy between field and lab P removal results and should be taken into consideration
477 when designing bioretention systems for water quality improvement.

478 **Hydraulic Effects of DWTRs**

479 Our hydraulic detention time and peak flow ratio results indicate that DWTRs did not
480 affect bioretention system hydraulics in this study (Figures 6 and 7). DWTRs have been shown
481 to reduce the hydraulic conductivity of bioretention media in laboratory column studies (Ament
482 et al. 2021; Yan et al. 2017). However, DWTRs were not expected to impact flow in this study
483 because the mixed DWTR layering strategy implemented here was shown to mitigate potential
484 hydraulic restrictions imposed by DWTRs in Ament et al. (2021). Additionally, the UNH
485 DWTRs exhibited higher hydraulic conductivity and coarser texture than sand in Ament et al.
486 (2021), so incorporating them into a sand-based media would place minimal restrictions on water
487 flow. Nevertheless, hydraulic concerns can limit the use of P-sorbing amendments in
488 bioretention systems (Liu and Davis 2014; Marvin et al. 2020; Penn and Bowen 2018; Poor et al.
489 2018; Yan et al. 2017) and have not been directly evaluated for DWTRs in field studies. These
490 results show that some DWTR sources can be used in bioretention systems to enhance P removal
491 without undermining hydraulic functions. More studies are needed to determine whether mixing
492 DWTRs with sand can alleviate hydraulic constraints imposed by very fine-grained, low
493 hydraulic conductivity DWTRs in the field.

494 The center of mass method for quantifying hydraulic detention time can produce
495 inaccurate results when applied to irregular, multimodal storm hydrographs (Barfield et al.
496 1981). Irregular hydrographs are common in small, flashy watersheds that exhibit short time of
497 concentration values. Consequently, the hydraulic detention time values reported in this study
498 likely do not reflect the true detention time of water in the bioretention systems. However, they

499 do reflect the relative differences in hydraulic detention time between the bioretention cells
500 monitored in this study and demonstrate that the DWTR used did not produce prolonged
501 detention times that can lead to excessive ponding and flooding.

502 **Impact of DWTRs on Heavy Metal Dynamics**

503 The presence of DWTRs did not affect heavy metal adsorption or leaching dynamics in
504 this bioretention study. Influent concentrations of all heavy metals were very low, which
505 prevented assessments of DWTR adsorption for As and Cd. Some evidence of Zn removal was
506 observed in this study, but these results were not unique to the DWTR cells and may be due to
507 Zn adsorption by organic media constituents (Davis et al. 2003; Li and Davis 2008). Effluent
508 concentrations of As, Cd and Zn were below the detection limit for all water samples, indicating
509 that the DWTRs and other bioretention media components used in this study did not leach these
510 metals during the monitored storms. Effluent concentrations of Mn were also below the detection
511 limit for all water samples, which is noteworthy because Mn leaching from DWTRs has been
512 identified as an environmental concern (Ippolito et al. 2011; Novak et al. 2007; Wang et al.
513 2014). All bioretention cells exhibited higher (but not statistically different) concentrations of Al
514 in effluent than influent (Figure 8a). The observation of minor Al leaching from all four cells
515 suggests that the sand, compost and gravel constituents of the media contribute a small amount
516 of Al to effluent loads. However, effluent concentrations of Al in this study averaged 0.028 mg
517 Al L⁻¹, which is far below the normalized chronic toxicity values for most aquatic species (U.S.
518 EPA 2018), and therefore likely would not threaten aquatic organisms in receiving waters.
519 Overall, these heavy metal results suggest that relatively small quantities of the DWTRs used
520 here can be incorporated into bioretention media to enhance P removal without posing toxicity

521 risks to downstream waterbodies. Further research is needed to determine variability in metals
522 leaching risk among DWTRs from different sources.

523 **Bioretention Media Design Implications**

524 The observation of significant SRP concentration reductions by DWTR media in both
525 this study and the preceding column study (Ament et al. 2021) highlight critical media design
526 factors for achieving P removal with DWTRs in bioretention systems. In this study, media
527 mixtures were created for two distinct bioretention layers: a 30.5 cm deep upper layer composed
528 of 10% low P compost and 90% washed sand (by volume), and a 30.5 cm deep lower layer
529 composed of 10% DWTR and 90% washed sand (by volume) (Figure 1). However, Liu and
530 Davis (2014) rotated 5% DWTR by mass into the top 40 cm of a 50-80 cm deep existing sandy
531 loam media and Houle (2017) mixed 10% DWTR by volume into a media blend composed of
532 50% sand, 10% compost (derive from food and yard waste), and 20% woodchips.

533 The differences in media composition, layering strategy, and DWTR incorporation
534 techniques among these studies could account for their different SRP removal performance. For
535 example, the bioretention media of previous studies likely contained larger internal P pools than
536 the media used in the current study due to their relative ages (Liu and Davis 2014) or organic
537 matter content (Houle 2017). Leaching from these P pools may have prematurely saturated the
538 DWTRs and prevented them from removing SRP from stormwater. Moreover, DWTRs were
539 placed below organic media constituents (e.g. compost, organic sediments, plant litter) in this
540 study, allowing them to bind dissolved P leaching downward from surface layers. Previous field
541 studies either incorporated DWTRs into the top of existing media (Liu and Davis 2014) or mixed
542 them uniformly with organic components within a media blend (Houle 2017), which may have
543 spatially prevented DWTRs from sorbing all internal sources of P. Finally, previous studies

544 incorporated DWTRs into bioretention media using backhoes (Roseen and Stone 2013), and
545 noted that such mixing strategies could have produced clumpy, heterogenous media that
546 facilitated preferential flow paths. Sieving the DWTRs and blending the media layers with
547 motorized cement mixers in this study may have produced a more homogenous media that
548 enabled effective P removal by allowing stormwater to fully contact the soil media.

549 Although DWTRs have large P sorption capacities, comparisons between field studies
550 suggest that they must be strategically incorporated into bioretention media to achieve their
551 maximum P removal potential. Compost selection criteria, media layering strategies, and DWTR
552 incorporation techniques appear to exert strong control over the P removal efficacy of DWTRs in
553 bioretention systems.

554 CONCLUSION

555 This is the first field study to clearly demonstrate that additions of DWTRs to
556 bioretention media can increase dissolved P removal from urban stormwater. Rather than P loads
557 being managed through stormwater volume reductions alone, this research observed P load
558 reductions that were driven by P concentration reductions, which played a greater role in P
559 removal for the DWTR cells. Differences in P removal performance between the Control and
560 DWTR cells were most pronounced during large storm events, which contributed
561 disproportionately to annual P loads. Growing differences in SRP removal between the Control
562 and DWTR cells suggests that the demonstrated capacity of DWTRs to enhance P removal is
563 conservative in this study, and that performance gaps between the DWTR media and Control
564 media are likely to expand over time. Notably, the Control media demonstrated excellent P
565 retention capacity relative to other field bioretention studies (Cording et al. 2018; Dietz and
566 Clausen 2005; Hunt et al. 2006; Paus et al. 2014; Shrestha et al. 2018), highlighting the

567 importance of compost selection criteria in bioretention media designs. Beyond P removal, the
568 addition of DWTRs to bioretention media had no impact on system hydraulics. Additionally, no
569 significant evidence of heavy metal leaching from, or adsorption by, DWTRs was observed in
570 this study. Media design decisions (e.g. compost amount and type, media layering strategy,
571 DWTR incorporation techniques and placement) appear to strongly influence the hydraulic
572 effects and P removal performance of DWTRs. More lab and field studies that examine different
573 DWTR materials and design strategies are needed to reduce uncertainty regarding performance
574 variability and to determine best practices for material testing prior to field use.

575 DATA AVAILABILITY STATEMENT

576 All data, models, or code that support the findings of this study are available from the
577 corresponding author upon reasonable request.

578 ACKNOWLEDGEMENTS

579 We thank Carl Betz, Nicholas Kaminski, Jillian Sarazen, Joshua Faulkner, and Daniel Needham
580 for assistance in the field and laboratory. Mark Voorhees and Eric Perkins of the United States
581 Environmental Protection Agency (U.S. EPA) contributed to conceptualizing this research. We
582 are grateful to James Houle of the University of New Hampshire Stormwater Center for providing
583 the DWTRs analyzed in this study. This research was supported by the U.S. EPA, Office of
584 Research and Development, in addressing EPA Region 1's needs and priorities in improving the
585 phosphorus removal efficiency of Green Infrastructure (bioretention media) as a Regional Applied
586 Research Effort (RARE) (project # 1937). Funding was made available to the University of
587 Vermont through an interagency agreement with the National Oceanic and Atmospheric
588 Administration (NOAA) National Sea Grant College Program Award NA18OAR4170099 to the
589 Lake Champlain Sea Grant Institute. Although this manuscript has been reviewed and approved

590 for publication by the Agencies, the views expressed in this manuscript are those of the authors
591 and do not necessarily represent the views or policies of the U.S. EPA or NOAA-Sea Grant. We
592 thank Drs. Brent Johnson and Heather Golden from the U.S. EPA ORD for their technical review
593 and valuable comments.

594 SUPPLEMENTAL MATERIALS

595 Figure S1 and Tables S1-S4 are available online in the ASCE Library (ascelibrary.org).

596 REFERENCES

- 597 Ament, M. R., Hurley, S. E., Voorhees, M., Perkins, E., Yuan, Y., Faulkner, J. W., and Roy, E.
598 D. (2021). “Balancing hydraulic control and phosphorus removal in bioretention media
599 amended with drinking water treatment residuals.” *ACS ES&T Water*, American Chemical
600 Society, 1(3), 688–697.
- 601 APHA, AWA, and WPCF. (2005). *Standard methods for the examination of water and*
602 *wastewater*. (American Public Health Association, ed.), American Environment
603 Association, Washington D.C. .
- 604 Babatunde, A. O., and Zhao, Y. Q. (2007). “Constructive approaches toward water treatment
605 works sludge management: An international review of beneficial reuses.” *Critical Reviews*
606 *in Environmental Science and Technology*, 37(2), 129–164.
- 607 Babatunde, A. O., Zhao, Y. Q., Burke, A. M., Morris, M. A., and Hanrahan, J. P. (2009).
608 “Characterization of aluminium-based water treatment residual for potential phosphorus
609 removal in engineered wetlands.” *Environmental Pollution*, 157(10), 2830–2836.
- 610 Barfield, B. J., Warner, R. C., and Haan, C. T. (1981). *Applied hydrology and sedimentology for*
611 *disturbed areas*. Oklahoma Technical Press.
- 612 Blecken, G. T., Zinger, Y., Deletić, A., Fletcher, T. D., and Viklander, M. (2009). “Influence of
613 intermittent wetting and drying conditions on heavy metal removal by stormwater
614 biofilters.” *Water Research*, Elsevier Ltd, 43(18), 4590–4598.
- 615 Buda, A. R., Koopmans, G. F., Bryant, R. B., and Chardon, W. J. (2012). “Emerging
616 technologies for removing nonpoint phosphorus from surface water and groundwater:
617 introduction.” *Journal of Environmental Quality*, American Society of Agronomy, 41(3),
618 621–627.
- 619 Carpenter, S. R., Caraco, N. F., Correll, D. L., Howarth, R. W., Sharpley, A. N., and Smith, V.
620 H. (1998). “Nonpoint pollution of surface waters with phosphorus and nitrogen.” *Ecological*
621 *Applications*, 8(3), 559–568.
- 622 Chahal, M. K., Shi, Z., and Flury, M. (2016). “Nutrient leaching and copper speciation in
623 compost-amended bioretention systems.” *Science of the Total Environment*, Elsevier B.V.,

624 556, 302–309.

625 Cording, A., Hurley, S., and Adair, C. (2018). “Influence of critical bioretention design factors
626 and projected increases in precipitation due to climate change on roadside bioretention
627 performance.” *Journal of Environmental Engineering*, American Society of Civil Engineers
628 (ASCE), 144(9), 04018082.

629 Cording, A., Hurley, S., and Whitney, D. (2017). “Monitoring methods and designs for
630 evaluating bioretention performance.” *Journal of Environmental Engineering (United
631 States)*, American Society of Civil Engineers (ASCE), 143(12).

632 Cucarella, V., and Renman, G. (2009). “Phosphorus sorption capacity of filter materials used for
633 on-site wastewater treatment determined in batch experiments—a comparative study.”
634 *Journal of Environment Quality*, American Society of Agronomy, 38(2), 381.

635 Davis, A. P. (2007). “Field performance of bioretention: water quality.” *Environmental
636 Engineering Science*, Mary Ann Liebert Inc, 24(8), 1048–1064.

637 Davis, A. P. (2008). “Field performance of bioretention: hydrology impacts.” *Journal of
638 Hydrologic Engineering*, American Society of Civil Engineers (ASCE), 13(2), 90–95.

639 Davis, A. P., Hunt, W. F., Traver, R. G., and Clar, M. (2009). “Bioretention technology:
640 overview of current practice and future needs.” *Journal of Environmental Engineering*,
641 American Society of Civil Engineers (ASCE), 135(3), 109–117.

642 Davis, A. P., Shokouhian, M., and Ni, S. (2001). “Loading estimates of lead, copper, cadmium,
643 and zinc in urban runoff from specific sources.” *Chemosphere*, Pergamon, 44(5), 997–1009.

644 Davis, A. P., Shokouhian, M., Sharma, H., Minami, C., and Winogradoff, D. (2003). “Water
645 quality improvement through bioretention: lead, copper, and zinc removal.” *Water
646 Environment Research*, Wiley, 75(1), 73–82.

647 Dietz, M. E., and Clausen, J. C. (2005). “A field evaluation of rain garden flow and pollutant
648 treatment.” *Water, Air, and Soil Pollution*, 167(1–4), 123–138.

649 Dunne, T., and Leopold, L. B. (1978). *Water in Environmental Planning*. Freeman, New York.

650 Grebel, J. E., Mohanty, S. K., Torkelson, A. A., Boehm, A. B., Higgins, C. P., Maxwell, R. M.,
651 Nelson, K. L., and Sedlak, D. L. (2013). “Engineered infiltration systems for urban
652 stormwater reclamation.” *Environmental Engineering Science*, Mary Ann Liebert Inc,
653 30(8), 437–454.

654 Hatt, B. E., Fletcher, T. D., and Deletic, A. (2009). “Hydrologic and pollutant removal
655 performance of stormwater biofiltration systems at the field scale.” *Journal of Hydrology*,
656 Elsevier, 365(3–4), 310–321.

657 Hobbie, S. E., Finlay, J. C., Janke, B. D., Nidzgorski, D. A., Millet, D. B., and Baker, L. A.
658 (2017). “Contrasting nitrogen and phosphorus budgets in urban watersheds and implications
659 for managing urban water pollution.” *Proceedings of the National Academy of Sciences*,
660 114(16), 4177–4182.

661 Houle, J. (2017). “Performance analysis of two relatively small capacity urban retrofit

662 stormwater controls.” *Water Environment Federation Technical Exhibition and Conference*
663 *2017, WEFTEC 2017*, Water Environment Federation, 4013–4021.

664 Hunt, W. F., Jarrett, A. R., Smith, J. T., and Sharkey, L. J. (2006). “Evaluating bioretention
665 hydrology and nutrient removal at three field sites in North Carolina.” *Journal of Irrigation*
666 *and Drainage Engineering*, American Society of Civil Engineers (ASCE), 132(6), 600–608.

667 Hurley, S., Shrestha, P., and Cording, A. (2017). “Nutrient leaching from compost: implications
668 for bioretention and other green stormwater infrastructure.” *Journal of Sustainable Water in*
669 *the Built Environment*, 3(3), 04017006.

670 Ippolito, J. A., Barbarick, K. A., and Elliott, H. A. (2011). “Drinking water treatment residuals: a
671 review of recent uses.” *Journal of Environmental Quality*, American Society of Agronomy,
672 40(1), 1–12.

673 Komlos, J., and Traver, R. G. (2012). “Long-term orthophosphate removal in a field-scale storm-
674 water bioinfiltration rain garden.” *Journal of Environmental Engineering*, American Society
675 of Civil Engineers (ASCE), 138(10), 991–998.

676 Leader, J. W., Dunne, E. J., and Reddy, K. R. (2008). “Phosphorus sorbing materials: sorption
677 dynamics and physicochemical characteristics.” *Journal of Environmental Quality*,
678 American Society of Agronomy, 37(1), 174–181.

679 LeFevre, G. H., Paus, K. H., Natarajan, P., Gulliver, J. S., Novak, P. J., and Hozalski, R. M.
680 (2015). “Review of dissolved pollutants in urban storm water and their removal and fate in
681 bioretention cells.” *Journal of Environmental Engineering*, American Society of Civil
682 Engineers (ASCE), 141(1), 04014050.

683 Li, H., and Davis, A. P. (2008). “Heavy metal capture and accumulation in bioretention media.”
684 *Environmental Science and Technology*, 42(14), 5247–5253.

685 Li, H., and Davis, A. P. (2009). “Water quality improvement through reductions of pollutant
686 loads using bioretention.” *Journal of Environmental Engineering*, American Society of
687 Civil Engineers (ASCE), 135(8), 567–576.

688 Li, J., and Davis, A. P. (2016). “A unified look at phosphorus treatment using bioretention.”
689 *Water Research*, Elsevier Ltd, 90, 141–155.

690 Li, M., Liu, J., Xu, Y., Qian, G., Li, M., and Xu, Y. (2016). “Phosphate adsorption on metal
691 oxides and metal hydroxides : A comparative review.” *Environmental Reviews*, 332(May),
692 1–58.

693 Lim, H. S., Lim, W., Hu, J. Y., Ziegler, A., and Ong, S. L. (2015). “Comparison of filter media
694 materials for heavy metal removal from urban stormwater runoff using biofiltration
695 systems.” *Journal of Environmental Management*, Academic Press, 147, 24–33.

696 Liu, J., and Davis, A. P. (2014). “Phosphorus speciation and treatment using enhanced
697 phosphorus removal bioretention.” *Environmental Science & Technology*, American
698 Chemical Society, 48(1), 607–614.

699 Liu, J., Sample, D. J., Owen, J. S., Li, J., and Evanylo, G. (2014). “Assessment of selected
700 bioretention blends for nutrient retention using mesocosm experiments.” *Journal of*

701 *Environmental Quality*, American Society of Agronomy, 43(5), 1754–1763.

702 Liu, Y., Engel, B. A., Flanagan, D. C., Gitau, M. W., McMillan, S. K., and Chaubey, I. (2017).
703 “A review on effectiveness of best management practices in improving hydrology and water
704 quality: Needs and opportunities.” *Science of the Total Environment*, Elsevier B.V.

705 Lucas, W. C., and Greenway, M. (2011). “Phosphorus retention by bioretention mesocosms
706 using media formulated for phosphorus sorption: response to accelerated loads.” *Journal of*
707 *Irrigation and Drainage Engineering*, 137(3), 144–153.

708 Marvin, J. T., Passeport, E., and Drake, J. (2020). “State-of-the-art review of phosphorus
709 sorption amendments in bioretention media: a systematic literature review.” *Journal of*
710 *Sustainable Water in the Built Environment*, American Society of Civil Engineers (ASCE),
711 6(1), 03119001.

712 Mortula, M. M., and Gagnon, G. A. (2007). “Phosphorus treatment of secondary municipal
713 effluent using oven-dried alum residual.” *Journal of Environmental Science and Health,*
714 *Part A*, 42(11), 1685–1691.

715 Muerdter, C., Özkök, E., Li, L., and Davis, A. P. (2016). “Vegetation and media characteristics
716 of an effective bioretention cell.” *Journal of Sustainable Water in the Built Environment,*
717 American Society of Civil Engineers (ASCE), 2(1), 04015008.

718 Muerdter, C. P., Wong, C. K., and LeFevre, G. H. (2018). “Emerging investigator series: the role
719 of vegetation in bioretention for stormwater treatment in the built environment: pollutant
720 removal, hydrologic function, and ancillary benefits.” *Environmental Science: Water*
721 *Research & Technology*, Royal Society of Chemistry, 4(5), 592–612.

722 Mullane, J. M., Flury, M., Iqbal, H., Freeze, P. M., Hinman, C., Cogger, C. G., and Shi, Z.
723 (2015). “Intermittent rainstorms cause pulses of nitrogen, phosphorus, and copper in
724 leachate from compost in bioretention systems.” *Science of The Total Environment,*
725 Elsevier, 537, 294–303.

726 Müller, A., Österlund, H., Marsalek, J., and Viklander, M. (2020). “The pollution conveyed by
727 urban runoff: A review of sources.” *Science of The Total Environment*, Elsevier B.V., 709,
728 136125.

729 National Research Council. (2009). *Urban Stormwater Management in the United States.*
730 Washington, D.C.

731 Novak, J. M., Szogi, A. A., Watts, D. W., and Busscher, W. J. (2007). “Water treatment residuals
732 amended soils release Mn, Na, S, and C.” *Soil Science*, 172(12), 992–1000.

733 O’Neill, S. W., and Davis, A. P. (2011a). “Water treatment residual as a bioretention amendment
734 for phosphorus. I: Evaluation Studies.” *Journal of Environmental Engineering*, American
735 Society of Civil Engineers (ASCE), 138(3), 318–327.

736 O’Neill, S. W., and Davis, A. P. (2011b). “Water treatment residual as a bioretention amendment
737 for phosphorus. II: Long-Term Column Studies.” *Journal of Environmental Engineering,*
738 American Society of Civil Engineers (ASCE), 138(3), 328–336.

739 Palmer, E. T., Poor, C. J., Hinman, C., and Stark, J. D. (2013). “Nitrate and phosphate removal

740 through enhanced bioretention media: mesocosm study.” *Water Environment Research*,
741 Wiley, 85(9), 823–832.

742 Passeport, E., Hunt, W. F., Line, D. E., Smith, R. A., and Brown, R. A. (2009). “Field study of
743 the ability of two grassed bioretention cells to reduce storm-water runoff pollution.” *Journal*
744 *of Irrigation and Drainage Engineering*, American Society of Civil Engineers (ASCE),
745 135(4), 505–510.

746 Paus, K. H., Morgan, J., Gulliver, J. S., and Hozalski, R. M. (2014). “Effects of bioretention
747 media compost volume fraction on toxic metals removal, hydraulic conductivity, and
748 phosphorous release.” *Journal of Environmental Engineering*, American Society of Civil
749 Engineers (ASCE), 140(10), 04014033.

750 Penn, C. J., and Bowen, J. M. (2018). *Design and Construction of Phosphorus Removal*
751 *Structures for Improving Water Quality*. Springer International Publishing, Cham.

752 Poor, C. J., Conkle, K., MacDonald, A., and Duncan, K. (2018). “Water treatment residuals in
753 bioretention planters to reduce phosphorus levels in stormwater.” *Environmental*
754 *Engineering Science*, Mary Ann Liebert Inc, 36(3), 265–272.

755 R Core Team. (2016). “R: A language and environment for statistical computing.” Vienna,
756 Austria.

757 Roseen, R. M., and Stone, R. M. (2013). *Evaluation and Optimization of Bioretention Design for*
758 *Nitrogen and Phosphorus Removal*. University of New Hampshire Stormwater Center,
759 Durham, NH.

760 Schlesinger, W. H., and Bernhardt, E. (2013). *Biogeochemistry: An Analysis of Global Change*.

761 Shrestha, P., Faulkner, J. W., Kokkinos, J., and Hurley, S. E. (2020). “Influence of low-
762 phosphorus compost and vegetation in bioretention for nutrient and sediment control in
763 runoff from a dairy farm production area.” *Ecological Engineering*, Elsevier B.V., 150.

764 Shrestha, P., Hurley, S. E., and Wemple, B. C. (2018). “Effects of different soil media,
765 vegetation, and hydrologic treatments on nutrient and sediment removal in roadside
766 bioretention systems.” *Ecological Engineering*, Elsevier B.V., 112, 116–131.

767 Siswoyo, E., Mihara, Y., and Tanaka, S. (2014). “Determination of key components and
768 adsorption capacity of a low cost adsorbent based on sludge of drinking water treatment
769 plant to adsorb cadmium ion in water.” *Applied Clay Science*, Elsevier Ltd, 97–98, 146–
770 152.

771 Steele, M. K., McDowell, W. H., and Aitkenhead-Peterson, J. A. (2015). “Chemistry of urban,
772 suburban, and rural surface waters.” 297–339.

773 Taguchi, V., Weiss, P., Gulliver, J., Klein, M., Hozalski, R., Baker, L., Finlay, J., Keeler, B., and
774 Nieber, J. (2020). “It is not easy being green: recognizing unintended consequences of green
775 stormwater infrastructure.” *Water*, MDPI AG, 12(2), 522.

776 Tirpak, R. A., Afrooz, A. N., Winston, R. J., Valenca, R., Schiff, K., and Mohanty, S. K. (2021).
777 “Conventional and amended bioretention soil media for targeted pollutant treatment: A
778 critical review to guide the state of the practice.” *Water Research*, Elsevier Ltd, 189,

779 116648.

780 U.S. EPA. (1999). *Preliminary Data Summary of Urban Storm Water Best Management*
781 *Practices*.

782 U.S. EPA. (2009). *National Water Quality Inventory : Report to Congress - 2004 Reporting*
783 *Cycle*. Washington, D.C.

784 U.S. EPA. (2018). *Aquatic Life Criteria for Aluminum in Freshwater*.

785 Vijayaraghavan, K., Biswal, B. K., Adam, M. G., Soh, S. H., Tsen-Tieng, D. L., Davis, A. P.,
786 Chew, S. H., Tan, P. Y., Babovic, V., and Balasubramanian, R. (2021). “Bioretention
787 systems for stormwater management: Recent advances and future prospects.” *Journal of*
788 *Environmental Management*, Academic Press, 292, 112766.

789 Wang, C., Bai, L., Pei, Y., and Wendling, L. A. (2014). “Comparison of metals extractability
790 from Al/Fe-based drinking water treatment residuals.” *Environmental Science and Pollution*
791 *Research*, Springer Verlag, 21(23), 13528–13538.

792 Winston, R. J., Hunt, W. F., Kennedy, S. G., Merriman, L. S., Chandler, J., and Brown, D.
793 (2013). “Evaluation of floating treatment wetlands as retrofits to existing stormwater
794 retention ponds.” *Ecological Engineering*, Elsevier, 54, 254–265.

795 Yan, Q., Davis, A. P., and James, B. R. (2016a). “Enhanced organic phosphorus sorption from
796 urban stormwater using modified bioretention media: batch studies.” *Journal of*
797 *Environmental Engineering*, American Society of Civil Engineers, 142(4), 04016001.

798 Yan, Q., James, B. R., and Davis, A. P. (2016b). “Lab-scale column studies for enhanced
799 phosphorus sorption from synthetic urban stormwater using modified bioretention media.”
800 *Journal of Environmental Engineering*, American Society of Civil Engineers (ASCE),
801 143(1), 04016073.

802 Yan, Q., James, B. R., and Davis, A. P. (2017). “Bioretention media for enhanced permeability
803 and phosphorus sorption from synthetic urban stormwater.” *Journal of Sustainable Water in*
804 *the Built Environment*, American Society of Civil Engineers (ASCE), 4(1), 04017013.

805 Yang, Y., Tomlinson, D., Kennedy, S., and Zhao, Y. Q. (2006). “Dewatered alum sludge: a
806 potential adsorbent for phosphorus removal.” *Water Science and Technology*, 54(5), 207–
807 213.

808 Zhao, Y. Q., and Yang, Y. (2010). “Extending the use of dewatered alum sludge as a P-trapping
809 material in effluent purification: study on two separate water treatment sludges.” *Journal of*
810 *Environmental Science and Health - Part A Toxic/Hazardous Substances and*
811 *Environmental Engineering*, Taylor and Francis Inc., 45(10), 1234–1239.

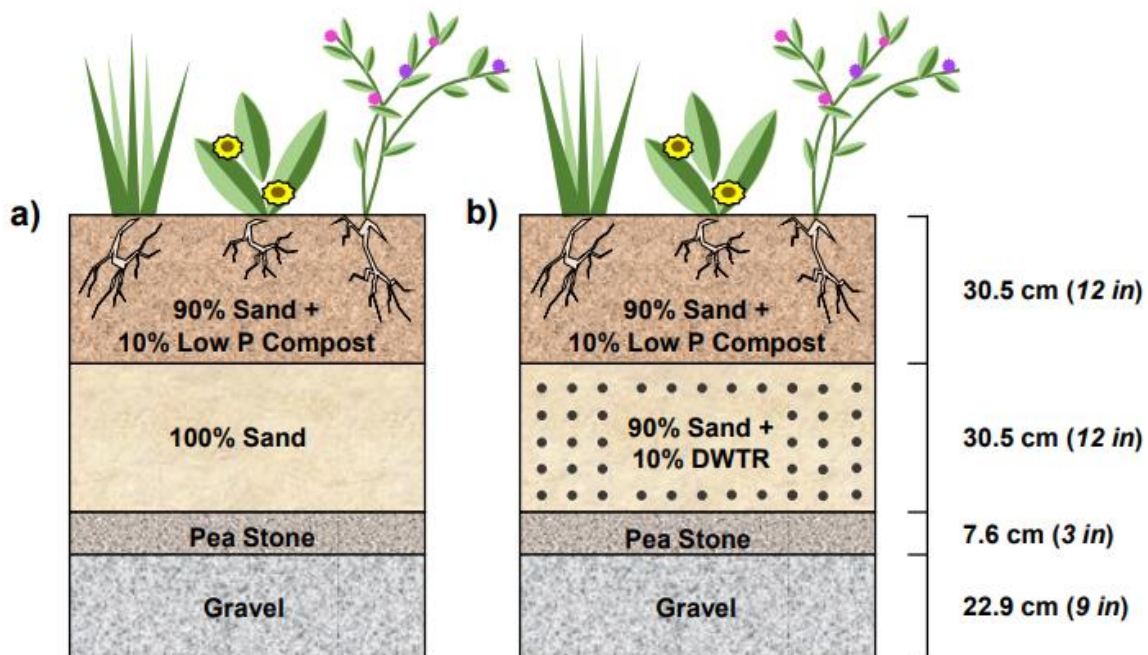
812 Zhou, Y.-F., and Haynes, R. J. (2012). “A comparison of water treatment sludge and red mud as
813 adsorbents of As and Se in aqueous solution and their capacity for desorption and
814 regeneration.” *Water, Air, & Soil Pollution*, 223(9), 5563–5573.

815 Zinger, Y., Prodanovic, V., Zhang, K., Fletcher, T. D., and Deletic, A. (2021). “The effect of
816 intermittent drying and wetting stormwater cycles on the nutrient removal performances of
817 two vegetated biofiltration designs.” *Chemosphere*, Elsevier Ltd, 267, 129294.

818 Zvomuya, F., Rosen, C. J., and Gupta, S. C. (2006). "Phosphorus sequestration by chemical
819 amendments to reduce leaching from wastewater applications." *Journal of Environmental*
820 *Quality*, Wiley, 35(1), 207–215.

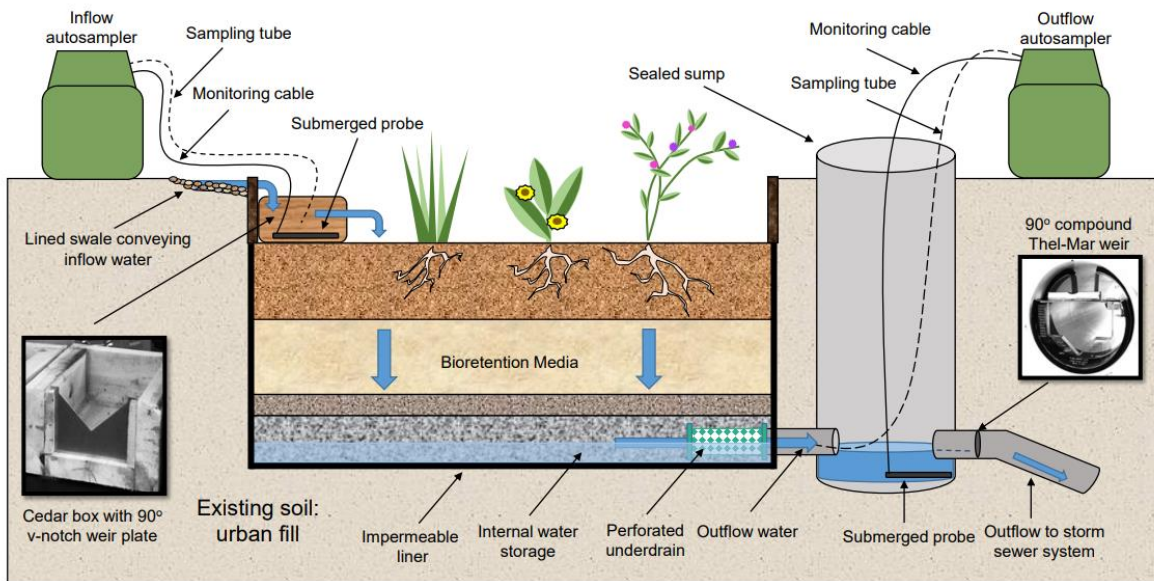
821

822 FIGURES



823

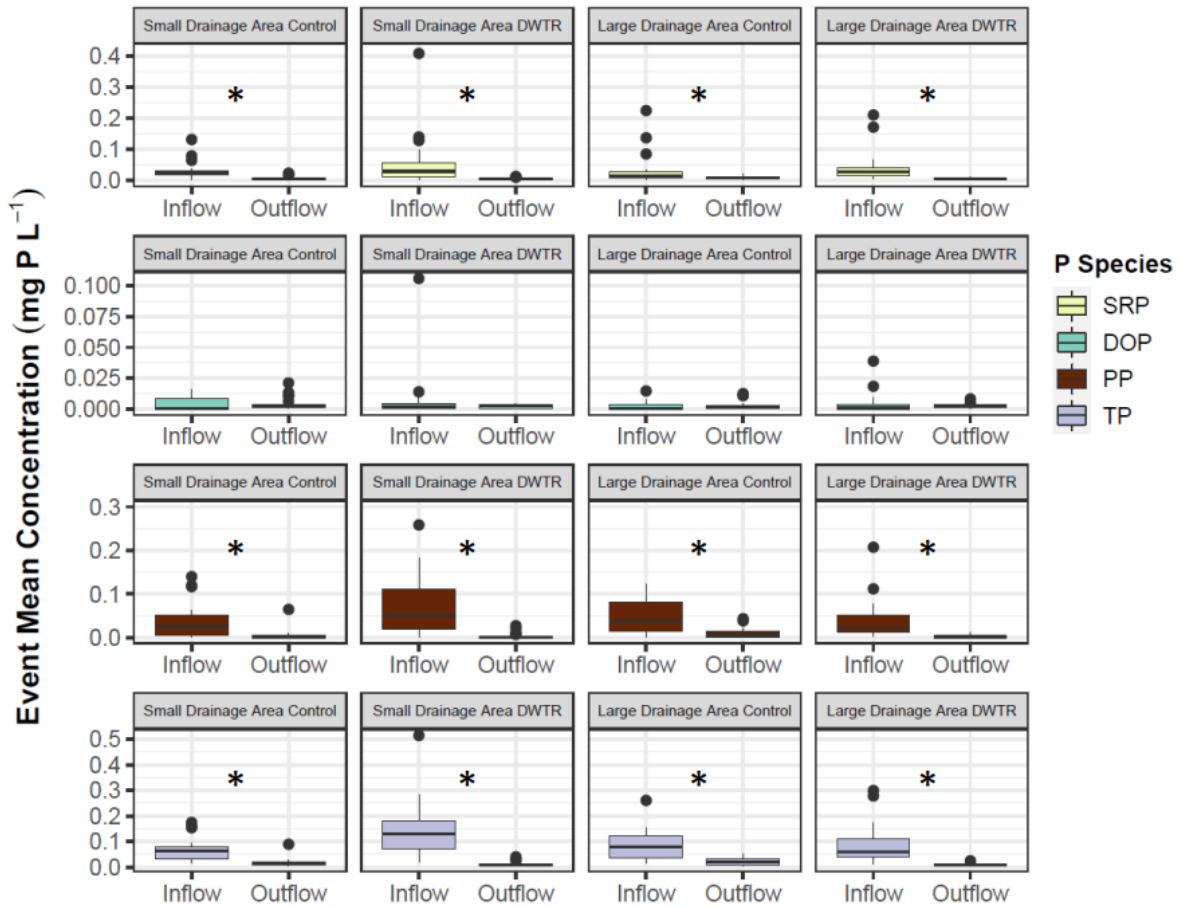
824 **Fig. 1.** Bioretention media profiles: a) Control media b) DWTR media



825

826 **Fig. 2.** Stormwater inflow and outflow monitoring systems. Weir photos are from Cording *et al.*

827 (2017).



828

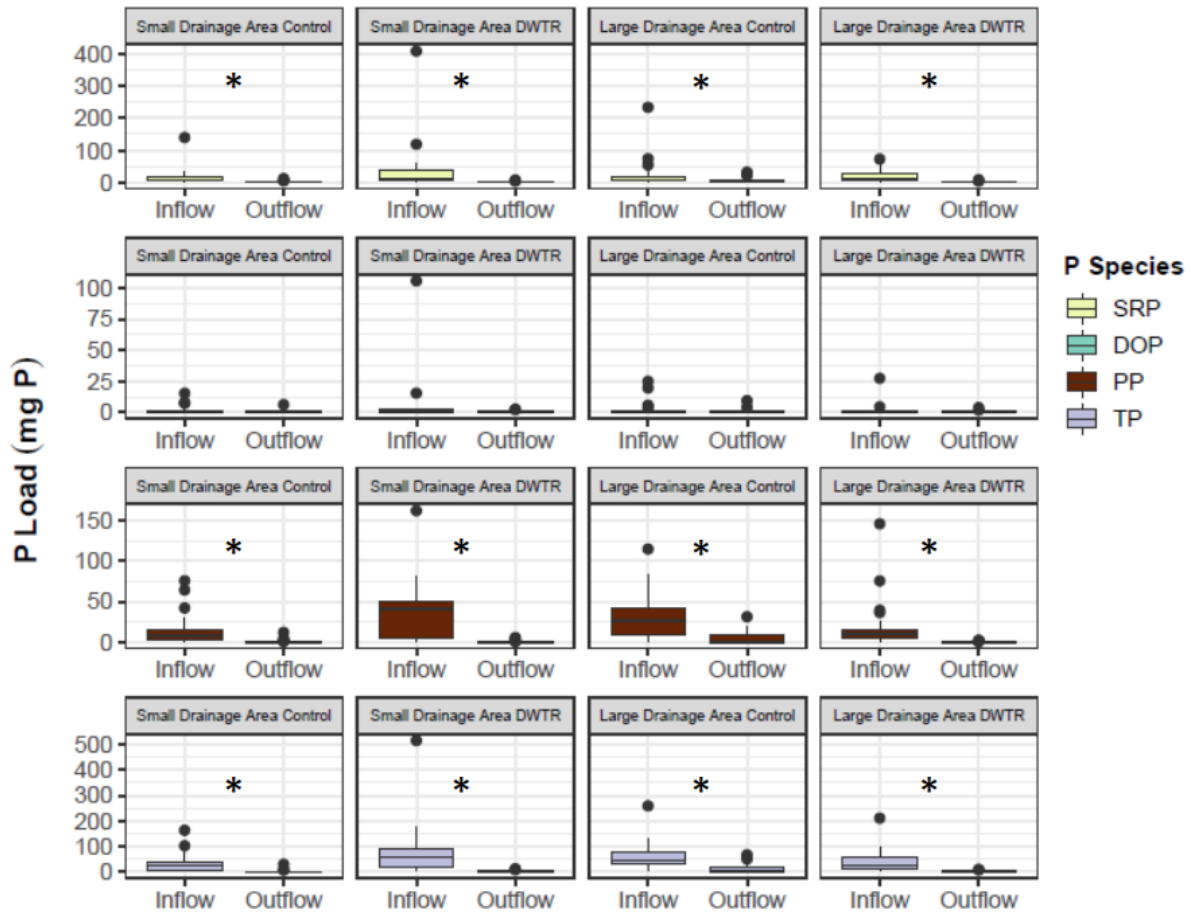
829 **Fig. 3.** Phosphorus (P) inflow and outflow event mean concentrations (EMC) for each
 830 bioretention cell and P species. Box and whisker plots represent the distribution of EMC inflow
 831 and outflow data for soluble reactive P (SRP), dissolve organic P (DOP), particulate P (PP), and
 832 total P (TP) during all storm events captured during the 2019 and 2020 monitoring seasons ($n =$
 833 21). Asterisks (*) between bars denote significant differences between inflow and outflow
 834 EMCs ($\alpha = 0.05$). Note that the y-axes differ between P species.

835

836

837

838



839

840 **Fig. 4.** Phosphorus (P) inflow and outflow mass loads for each bioretention cell and P species.

841 Box and whisker plots represent the distribution of inflow and outflow P load data for soluble

842 reactive P (SRP), dissolved organic P (DOP), particulate P (PP), and total P (TP) for all storm

843 events captured during the 2019 and 2020 monitoring seasons ($n = 21$). Asterisks (*) between

844 bars denote significant differences between inflow and outflow P loads ($\alpha = 0.05$). Note that the

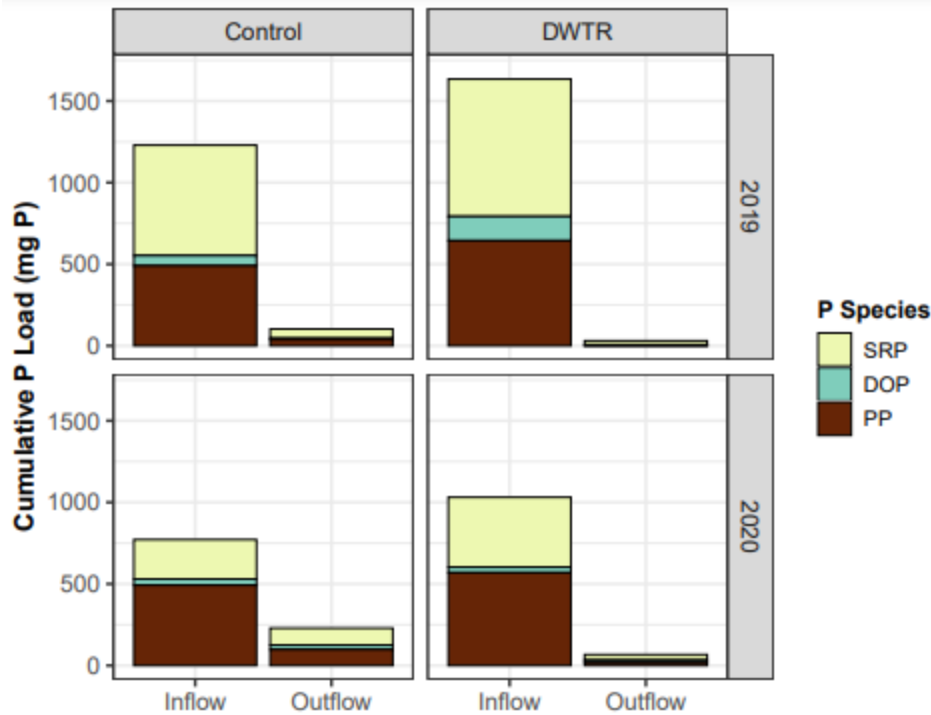
845 y-axes differ between P species.

846

847

848

849



850

851 **Fig. 5.** Phosphorus (P) inflow and outflow loads for the Control media (2 bioretention cells) and
 852 drinking water treatment residual (DWTR) media (2 bioretention cells) cells. Bars represent the
 853 cumulative sum of loads captured in each of the media treatments during the 2019 (September-
 854 November; $n=8$ storms) and 2020 (June-November; $n=13$ storms) monitoring seasons for soluble
 855 reactive P (SRP), dissolved organic P (DOP), and particulate P (PP). The summed height of the
 856 stacked bars represents the total P (TP) load for each media treatment and monitoring season.

857

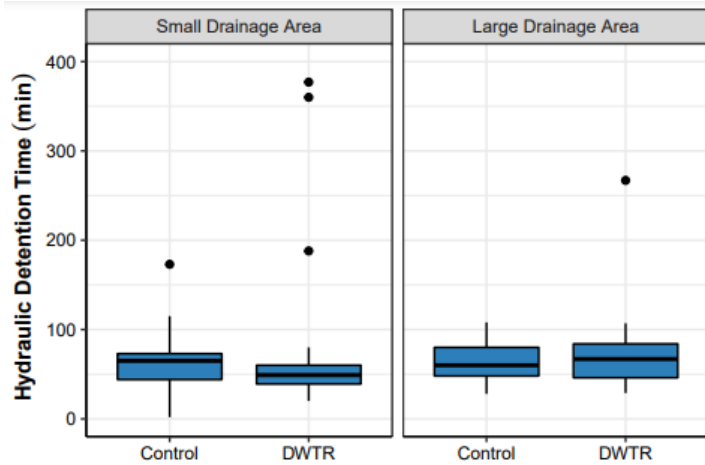
858

859

860

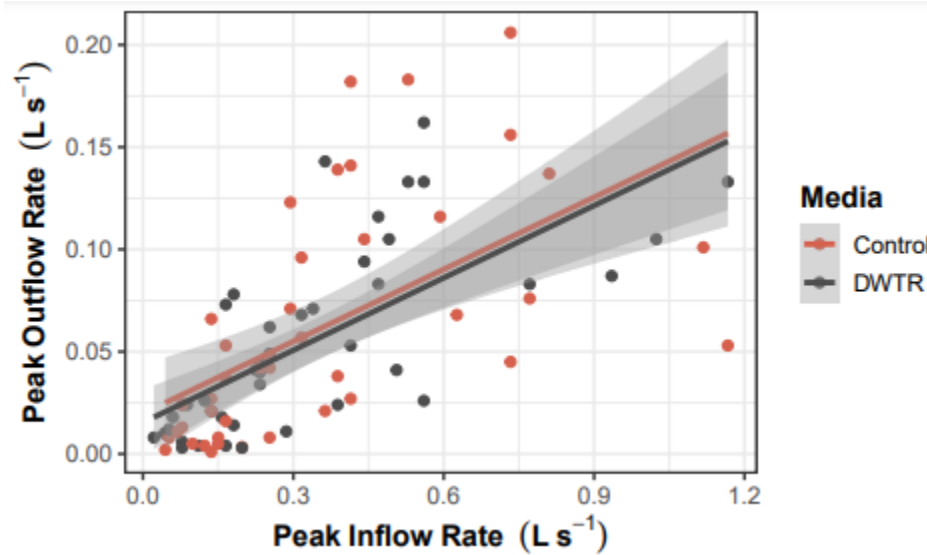
861

862



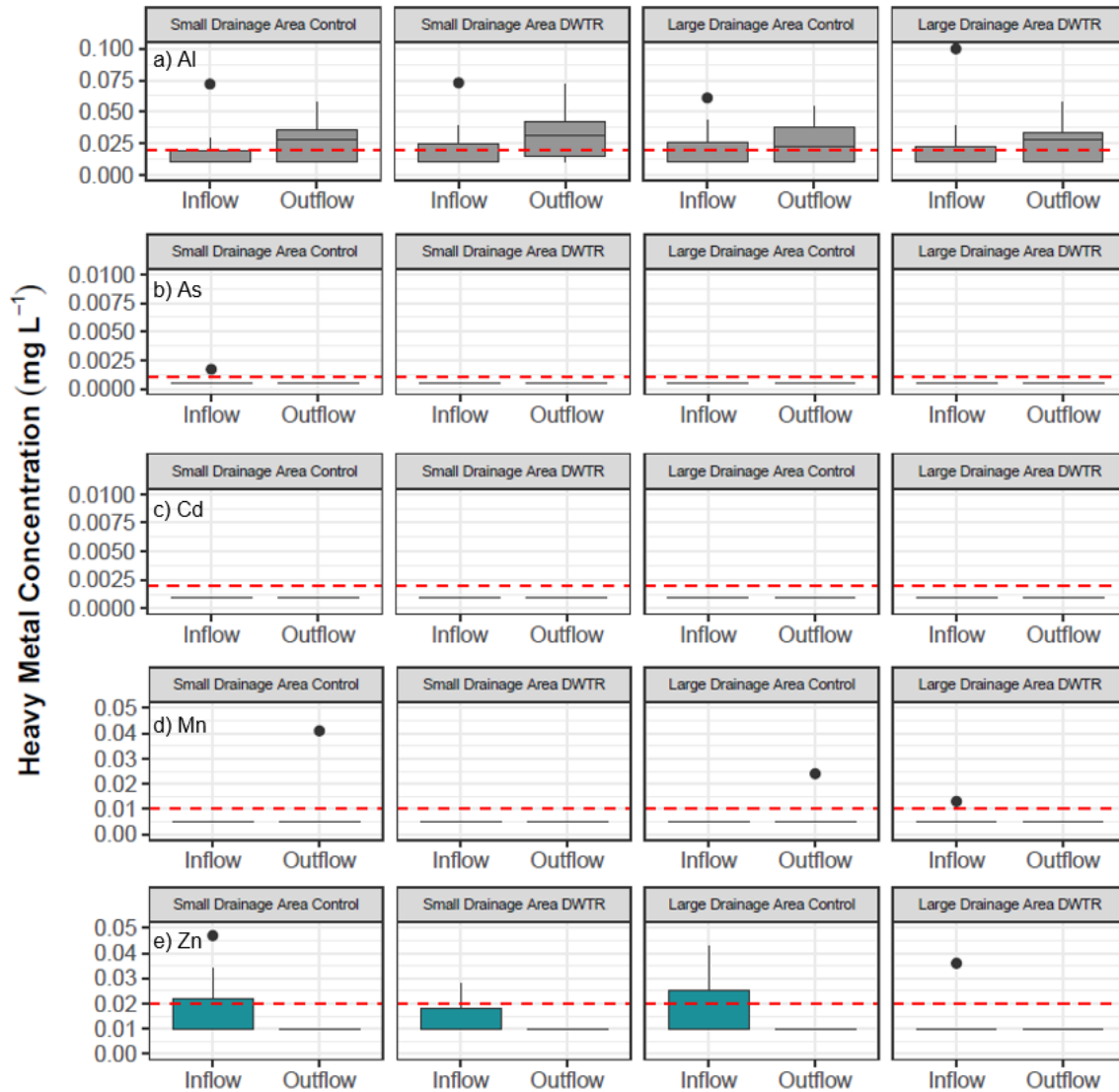
863

864 **Fig. 6.** Hydraulic detention times for each bioretention cell. Box and whisker plots represent the
 865 distribution of detention times observed during all storms captured in the 2019 and 2020
 866 monitoring seasons ($n = 21$).



867

868 **Fig. 7.** Peak inflow and peak outflow rates from the Control media (2 bioretention cells) and
 869 drinking water treatment residual (DWTR) media (2 bioretention cells) for all storm events
 870 captured in the 2019 and 2020 monitoring seasons ($n = 21$). Shaded lines represent the least
 871 squares regression line and 95% confidence interval for each media treatment.



872

873 **Fig. 8.** Heavy metal inflow and outflow event mean concentrations (EMC) for each bioretention
 874 cell. Box and whisker plots represent the distribution of inflow and outflow EMC data for
 875 aluminum (Al), arsenic (As), cadmium (Cd), manganese (Mn), and zinc (Zn) during four storms
 876 captured in 2019 and six storms captured in 2020. Red dashed lines indicate the detection limit
 877 for each heavy metal specie. Note that the y-axes differ between metal species.

878

879

880 TABLES

881 **Table 1.** Summary of stormwater inflows and outflows for each bioretention cell. Phosphorus
882 (P) load values represent the cumulative mass (mg) of each P species contained within the
883 bioretention influent and effluent. Event mean concentration (EMC) values represent the average
884 EMC value for all monitored storm events. Stormwater volumes represent the cumulative
885 volume (L) of stormwater that entered and exited each bioretention cell. Removal efficiency
886 values (RE) indicate the percentage of each constituent removed by the bioretention cell.

887

888

889

890

891

892

893

894

895

896

897

898

899

900

901

Bioretention Cell	Constituent		2019			2020			2-Year Totals		
			Inflow	Outflow	RE	Inflow	Outflow	RE	Inflow	Outflow	RE
Small Drainage Area Control (43 m ² drainage area)	Stormwater	Volume (L)	13152	4310	67	23340	15422	34	36492	19733	46
	SRP	Load (mg)	232.3	8.6	96	130.8	25.8	80	363.2	34.4	91
		EMC (mg/L)	0.050	0.008	85	0.020	0.008	61	0.032	0.008	75
	DOP	Load (mg)	32.7	2.2	93	6.6	8.9	-36	39.3	11.1	72
		EMC (mg/L)	0.007	0.004	36	0.002	0.004	-93	0.004	0.004	-9
	PP	Load (mg)	191.5	0.0	100	134.1	20.5	85	325.5	20.5	94
		EMC (mg/L)	0.054	0.0	100	0.027	0.008	70	0.037	0.005	87
	TP	Load (mg)	456.5	10.8	98	271.5	55.3	80	728.0	66.1	91
EMC (mg/L)		0.110	0.012	89	0.050	0.020	59	0.073	0.017	77	
Small Drainage Area DWTR (32 m ² drainage area)	Stormwater	Volume (L)	14957	6400	57	28841	17581	39	43798	23981	45
	SRP	Load (mg)	576.8	10.1	98	274.2	19.7	93	851.0	29.7	97
		EMC (mg/L)	0.105	0.006	95	0.030	0.006	80	0.059	0.006	90
	DOP	Load (mg)	111.8	3.1	97	24.6	6.4	74	136.5	9.5	93
		EMC (mg/L)	0.015	0.002	86	0.003	0.002	53	0.008	0.002	77
	PP	Load (mg)	421.2	0.0	100	355.0	12.3	97	776.2	12.3	98
		EMC (mg/L)	0.106	0.0	100	0.056	0.006	90	0.075	0.004	95
	TP	Load (mg)	1109.8	13.2	99	653.7	38.3	94	1763.6	51.5	97
EMC (mg/L)		0.226	0.008	97	0.089	0.013	85	0.141	0.011	92	
Large Drainage Area Control (59 m ² drainage area)	Stormwater	Volume (L)	23743	17233	27	39340	29193	26	63083	46426	26
	SRP	Load (mg)	444.3	48.2	89	110.7	77.3	30	555.1	125.5	77
		EMC (mg/L)	0.068	0.010	86	0.012	0.010	18	0.034	0.010	71
	DOP	Load (mg)	29.9	5.6	81	31.6	19.2	39	61.4	24.8	60
		EMC (mg/L)	0.002	0.001	40	0.002	0.004	-59	0.002	0.003	-20
	PP	Load (mg)	298.6	38.1	87	357.8	77.1	78	656.4	115.3	82
		EMC (mg/L)	0.055	0.008	86	0.047	0.010	78	0.050	0.009	82
	TP	Load (mg)	772.8	92.0	88	500.1	173.6	65	1272.8	265.5	79
EMC (mg/L)		0.126	0.019	85	0.062	0.024	61	0.086	0.022	75	
Large Drainage Area DWTR (54 m ² drainage area)	Stormwater	Volume (L)	15267	7410	51	31313	15116	52	46580	22526	52
	SRP	Load (mg)	264.9	14.6	94	153.7	13.9	91	418.5	28.6	93
		EMC (mg/L)	0.080	0.006	92	0.021	0.005	75	0.044	0.006	87
	DOP	Load (mg)	36.7	2.8	92	9.7	7.6	21	46.4	10.4	77
		EMC (mg/L)	0.009	0.002	77	0.002	0.002	-18	0.005	0.002	53
	PP	Load (mg)	222.7	0.0	100	214.1	7.1	97	436.8	7.1	98
		EMC (mg/L)	0.054	0.0	100	0.033	0.004	88	0.041	0.002	94
	TP	Load (mg)	524.3	17.5	97	377.4	28.7	92	901.7	46.1	95
EMC (mg/L)		0.143	0.008	94	0.056	0.012	79	0.089	0.010	88	